

Piezoelectric Characterization of Individual Zinc Oxide Nanobelt Probed by Piezoresponse Force Microscope

Min-Hua Zhao,[†] Zhong-Lin Wang,[‡] and Scott X. Mao^{*†}

Department of Mechanical Engineering, University of Pittsburgh, Pittsburgh, Pennsylvania 15261, and School of Materials Science and Engineering, Georgia Institute of Technology, Atlanta, Georgia 30332

Received December 17, 2003; Revised Manuscript Received February 8, 2004

ABSTRACT

Piezoresponse force microscopy (PFM) is used to measure the effective piezoelectric coefficient (d_{33}) of an individual (0001) surface dominated zinc oxide nanobelt lying on a conductive surface. Based on references of bulk (0001) ZnO and x -cut quartz, the effective piezoelectric coefficient d_{33} of ZnO nanobelt is found to be frequency dependent and varies from 14.3 pm/V to 26.7 pm/V, which is much larger than that of the bulk (0001) ZnO of 9.93 pm/V. The results support the application of ZnO nanobelts as nanosensors and nanoactuators.

Zinc oxide is a semiconducting piezoelectric material that has been used in microelectromechanical systems (MEMS) as sensors and actuators¹ and in communications as surface acoustic wave (SAW) and thin-film bulk acoustic wave resonator (FBAR) devices.^{2–3} Quasi-one-dimensional ZnO nanobelts have been synthesized,⁴ and they have been used for the fabrication of field effect transistors,⁵ gas sensors,⁶ resonators,⁷ and nanocantilevers.⁸ These applications mainly utilize the semiconducting properties and geometrical shape and size offered by nanobelts. ZnO nanobelts dominated by different crystal surfaces have been synthesized. The most common growth direction of the nanobelt is along the c -axis [0001] or [01 $\bar{1}$ 0], with the top surface being (2 $\bar{1}$ 10) and side surface being (01 $\bar{1}$ 0) or (0001), respectively (Figures 1a and b).⁴ Growth of (0001) surface dominated nanobelts has to overcome an energy barrier due to surface polarization. Recently, free-standing piezoelectric ZnO nanobelts dominated by large (0001) top and bottom surfaces (Figure 1c) have been synthesized.⁹ Individual zinc oxide nanobelt is a promising piezoelectric material for nanosensor and nano-actuator applications due to its perfect single crystalline structure and that it is free of dislocation.

Investigating the piezoelectric properties of ZnO nanobelt using atomic force microscopy remains, however, a challenge because the sample's displacement due to the inverse piezoelectric effect by applying an electric field is on the order of picometers (pm). Several techniques,^{10–12} including scanning probe microscopy (SPM),^{13–17} have been employed

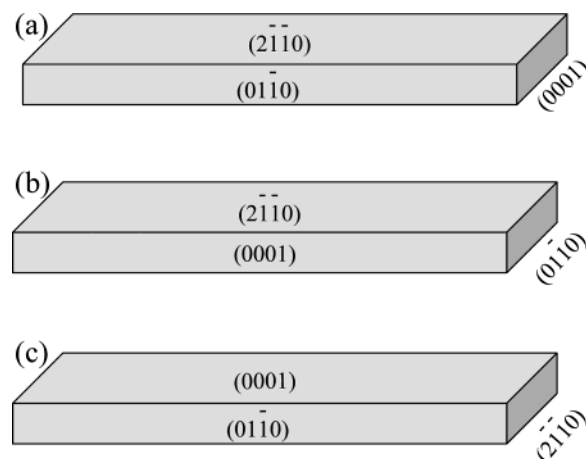


Figure 1. Surface facets of ZnO nanobelts: (A) growing along [0001] (c axis), top surfaces (2 $\bar{1}$ 10), and side surfaces (01 $\bar{1}$ 0), showing no piezoelectric property across thickness; (B) growing along [01 $\bar{1}$ 0] (c axis), top surfaces (2 $\bar{1}$ 10), and side surfaces (0001), showing no piezoelectric property across thickness; (C) growing along [2 $\bar{1}$ 10] (a axis), top surfaces (0001), and side surfaces (01 $\bar{1}$ 0), showing piezoelectric effect across thickness.

to measure these small piezoelectric displacements. In particular, piezoresponse force microscope (PFM) is becoming a standard method for the study of ferroelectric and piezoelectric phenomena. The PFM technique is based on the detection of local vibrations of a sample induced by an AC signal applied between the conductive tip of SFM and the bottom electrode of the sample. The local oscillations of the sample surface are transmitted to the tip and detected using a lock-in technique. The out-of-plane piezoresponse signal is extracted from the z -deflection signal given by the

* Corresponding author, Email: smao@engr.pitt.edu.

[†] University of Pittsburgh.

[‡] Georgia Institute of Technology.

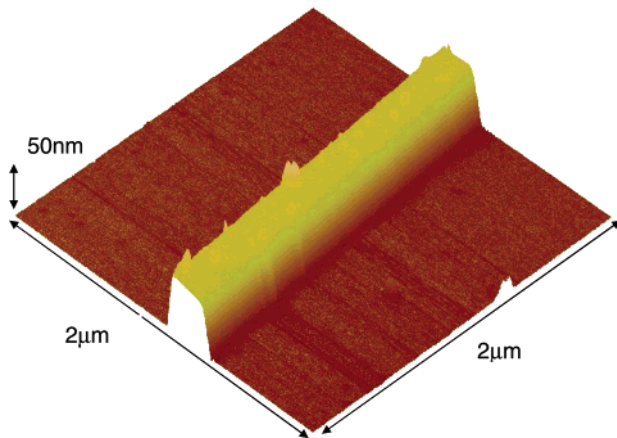


Figure 2. AFM 3D ($2\ \mu\text{m} \times 2\ \mu\text{m}$) image of an individual nanobelt (360 nm in width and 65 nm in thickness) lying on the substrate surface, showing a rectangular cross section.

PSD (position sensitive detector) and represents the local oscillations perpendicular to the plane of the sample surface. Though ferroelectric properties of individual barium titanate nanowires investigated by noncontact mode of SPM were reported by H. Park's group,¹⁵ there are no publications on piezoelectric measurement of one-dimensional nanostructures using the contact mode of SPM.

This paper reports our measurements of the piezoelectric properties of individual ZnO nanobelts using the PFM technique. The result is compared with that of the (0001) bulk ZnO and *x*-cut quartz. Our results show that the effective piezoelectric coefficient d_{33} for a ZnO nanobelt is significantly larger than that of bulk ZnO, establishing the basis for using ZnO nanobelts for nanoscale sensors and actuators.

The first step of the experiment was sample preparation. After coating (100) Si wafers with 100 nm Pd, ZnO nanobelts⁴ with typical dimension of tens of nanometers in thickness, hundreds of nanometers in width, and tens of micrometers in length were dispersed on the conductive surface similar to the method described previously.¹⁸ Then the whole surface was coated with another 5 nm Pd coating, which served as an electrode on the ZnO nanobelt to get a uniform electric field and avoid electrostatic effects.¹³ Extra care was taken to ensure that the top and bottom surface of the nanobelt was not short-circuited after Pd deposition.

The ZnO nanobelt was located by a commercially available AFM (Nanoscope IIIa, Multimode) in tapping mode. If contact mode was used, the nanobelt might be displaced by the tip during scanning, which causes a distorted image. Figure 2 is a three-dimensional image of an individual ZnO nanobelt lying on the surface as obtained in tapping mode, which clearly shows a rectangular cross section. After locating the nanobelt, the tip was positioned to the center of the nanobelt.

It is worth mentioning that not every nanobelt lying on the surface is piezoelectric. The nanobelt showing piezoelectric characteristics grows along $[2\bar{1}\bar{1}0]$ with a (0001) top surface, as presented in Figure 1c. The polar axis of the hexagonal wurtzite structured ZnO crystal is along [0001]. Piezoelectric measurements on the ZnO nanobelt were

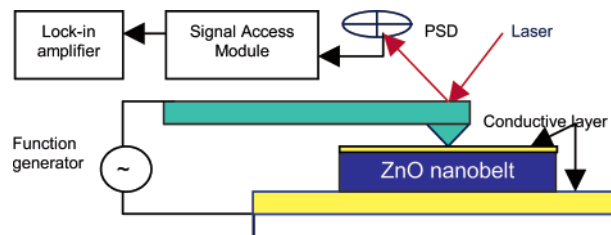


Figure 3. Schematic diagram of experimental setup.

performed in contact mode at a single point with the addition of a function generator, a lock-in amplifier (SR844), and a signal access module (SBOB) as shown in Figure 3.

In this configuration, the conductive tip supplies current to the electrode and also measures the piezoelectric motion. The conductive tip is made by coating Pd (20 nm thick) on a commercial Olympus etched silicon probe with nominal spring constant of 42 N/m and tip radius of about 10 nm. A high stiffness cantilever is chosen to reduce the influence of electrostatic interaction with piezoelectric measurement.^{13,17–19} The contact force between the AFM tip and nanobelt is ~ 1800 nN, which ensures that the measurement is in the so-called strong-indentation regime proposed by S. V. Kalinin and D. A. Bonnell,²⁰ as the piezoresponse in the strong-indentation regime is dominated by the d_{33} of the material. The typical resonance of the conductive tip is about 300 kHz. The frequency of the signal applied on the sample is from 30 kHz to 150 kHz, which is much higher than the low-pass cutoff frequency of the AFM topography feedback loop and lower than the cantilever resonance frequency. The frequency range chosen is far above the previously reported values on bulk or thin film samples, ranging from 1 to 16.7 kHz.^{13,14,16,17} The reason for this choice is the higher the applied frequency, the lower the noise signal level as predicted by Harnagea et al.,¹⁷ which is below 10^{-13} m in the chosen frequency range. The input signal was in the range of 1–4 V (RMS). The corresponding vertical deflection signal of the cantilever is recorded by lock-in amplifier through SBOB. By multiplying the deflection signal with the calibration constant of the photodetector sensitivity,¹³ the amplitude of the tip vibration is derived. The calibration constant is determined from the slope of the force–distance plot obtained after the scanner is calibrated using a standard grating. Since the scanner has been independently calibrated with a known step height, the vertical deflection signal is calibrated to the known vertical displacement. As illustrated in eq 1,^{13,17,14} the slope of the amplitude A_f versus the input signal U_f gives the effective piezoelectric coefficient d_{33}^{eff} .

$$A_f = V_f \delta = d_{33}^{\text{eff}} U_f \quad (1)$$

where A_f is vibration amplitude (in units of nm), V_f is vertical deflection signal of the cantilever (mV), δ is the calibration constant of the photodetector sensitivity (nm/V), and U_f is the amplitude of the testing ac voltage (V).

To ensure the reliability and accuracy of the measurement, effective piezoelectric coefficients of (0001) bulk ZnO and *x*-cut quartz (serving as a piezoelectric standard) were

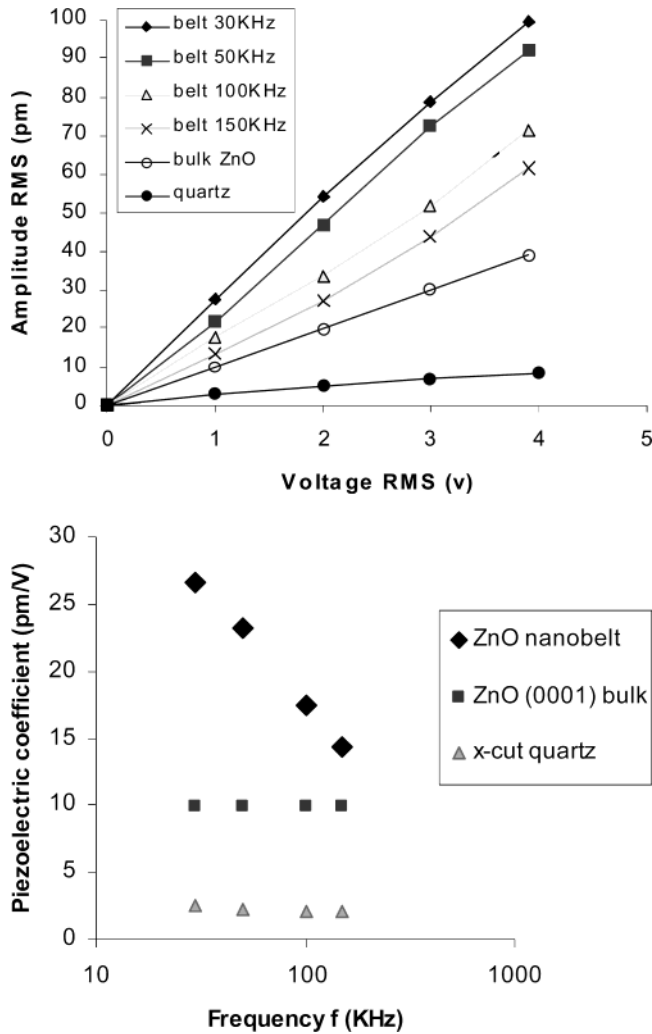


Figure 4. (a) Piezoelectric measurements of ZnO nanobelt, bulk (0001) ZnO, and *x*-cut quartz. The linear relationship between amplitude and applied voltage is shown in every case, the slope of which gives the piezoelectric coefficient. (b) Frequency dependence of piezoelectric coefficient of ZnO nanobelt, bulk (0001) ZnO, and *x*-cut quartz. Only the piezoelectric coefficient of ZnO nanobelt is frequency dependent.

measured using the same PFM technique. As to (0001) bulk ZnO ($5 \times 5 \times 0.5$ mm, supplied by M. T. I. Corp.), both sides were coated with 100 nm Pd and the bottom side was attached to the conductive surface using conductive epoxy. A similar process was applied to *x*-cut quartz ($\phi 10 \times 0.7$ mm, gold coating of 150 nm on each side, courtesy of Bliley Technologies Inc).

Experimental results of piezoelectric measurements on the ZnO nanobelt with (0001) top surface, (0001) ZnO bulk, and *x*-cut quartz are presented in Figure 4a. From the slopes of the curve, the effective piezoelectric coefficients are $d_{11} = 2.17$ pm/V for *x*-cut quartz and $d_{33} = 9.93$ pm/V for (0001) bulk ZnO, which are almost independent of frequency. Compared to the accepted values, $d_{11} = 2.3$ pm/V for quartz and $d_{33} = 12.4$ pm/V for ZnO,¹³ the measured results for ZnO bulk and *x*-cut quartz are reasonable, confirming the reliability and accuracy of the measuring technique. The effective piezoelectric coefficient of the ZnO nanobelt is frequency dependent and varies from 14.3 to 26.7 pm/V,

which is much larger than that of the bulk ZnO. One possible reason for the observed enhanced electromechanical response for the ZnO nanobelt might be due to its perfect single crystallinity and freedom of dislocation,⁴ as inherent reduction in the piezoelectric coefficient due to internal defects was revealed in ultrathin PZT films.²¹ As to a commercially available single-crystal bulk sample, a certain amount of defects were inevitable.

Next, an increase of piezoelectric response with decreasing feature size in epitaxial PZT thin film was reported by S. Buhlmann et al.²² The observed increase of piezoresponse amplitude was 300% with decreasing the film thickness from 200 to 100 nm, which was proposed to be mostly due to a change of domain configuration. Although this mechanism was not applicable to the ZnO nanobelt of tens of nanometer in thickness, the possible size effect of its piezoelectricity needs further investigation. Furthermore, the different elastic boundary condition in piezoelectric measurement on the ZnO nanobelt and bulk sample may contribute to the enhanced piezoelectric response. As to the ZnO nanobelt, there is no constraint at the interface between the bottom side and the conductive layer, while conductive epoxy is applied in the case of bulk sample. Hence, the effective piezoelectric coefficient of the ZnO nanobelt and bulk is given by eqs 2 and 3 using lateral free²³ and lateral full constraint²⁴ boundary conditions, respectively.

$$d_{33,\text{belt}}^{\text{eff}} \cong d_{33} \quad (2)$$

$$d_{33,\text{bulk}}^{\text{eff}} \cong d_{33} - \frac{2S_{13}}{S_{11} + S_{12}} d_{31} \quad (3)$$

Assuming that d_{33} is the same in eqs 2 and 3, it is interesting to estimate the magnitude of the second term in eq 3, which provides the effect of boundary condition. However, the components (S_{ij}) of compliance matrix (S) of ZnO are not directly available and are derived from the stiffness matrix C^{25} using the relationship $S = C^{-1}$.

$$S = \begin{bmatrix} 6.401 & -1.932 & -2.539 & 0 & 0 & 0 \\ -1.932 & 6.401 & -2.539 & 0 & 0 & 0 \\ -2.539 & -2.539 & 8.351 & 0 & 0 & 0 \\ 0 & 0 & 0 & 14 & 0 & 0 \\ 0 & 0 & 0 & 0 & 14 & 0 \\ 0 & 0 & 0 & 0 & 0 & 17 \end{bmatrix} \times 10^{-12} (\text{m}^2/\text{N}) \quad (4)$$

Using the S_{ij} value from eq 4 and $d_{31} = -5.1$ pm/V,¹⁹ we can estimate the second term in eq 3 to be 5.795 pm/V. Taking $d_{33} = 12.4$ pm/V (the accepted piezoelectric coefficient of single-crystal ZnO), we derive the conclusion that the boundary condition can change the effective piezoelectric coefficient of ZnO up to 47%.

The frequency dependence of the piezoelectric coefficient is shown in Figure 4b. Both ZnO bulk and *x*-cut quartz are almost frequency independent. As to the ZnO nanobelt, the higher the frequency (30–150 kHz), the lower the piezoelectric coefficient d_{33} , which depends linearly on the

logarithm of the applied field frequency. Such logarithmic frequency dependence was reported in ferroelectric materials such as PZT.^{26–27} Even though ZnO is not ferroelectric, the logarithmic frequency dependence is generally valid in random systems that have properties controlled by interface pinning,²⁷ such as pinning of spontaneous polarization in ZnO, which might be caused by surface charge due to the high surface-to-volume ratio of the ZnO nanobelt. Another possible reason for the unexpected frequency dependence might originate from the imperfect electrical contact between the bottom of the nanobelt and the conductive layer. With increasing the input frequency, the quality of electrical contact decreases, which induces the lower electromechanical response of the ZnO nanobelt.

In summary, the effective piezoelectric coefficient of the (0001) surface dominated ZnO nanobelt has been measured by PFM, and it is significantly larger than that of bulk (0001) ZnO. This is a very interesting property, illustrating the piezoelectric behavior of the (0001) surface-dominated ZnO nanobelt. The effective piezoelectric coefficient of the ZnO nanobelt is also frequency dependent, which may be due to the surface charge effect or imperfect electrical contact at the interface. The data presented here show that a ZnO nanobelt can be an excellent candidate for nanosensors and nanoactuators.

Acknowledgment. The authors are grateful for support from NSF Grant No. CMS-0140317 and NASA URETI.

References

- (1) Shibata, T.; Unno, K.; Makino, E.; Ito, Y.; Shimada, S. *Sens. Actuators A* **2002**, *102*, 106.
- (2) Kim, S. H.; Lee, J. S.; Choi, H. C.; Lee, Y. H. *IEEE Electron Dev. Lett.* **1999**, *20*, 113.

- (3) Molarius, J.; Kaitila, J.; Pensala, T.; Ylilammi, M. *J. Mater. Sci.* **2003**, *14*, 431.
- (4) Pan, Z. W.; Dai, Z. R.; Wang, Z. L. *Science* **2001**, *291*, 1947.
- (5) Arnold, M.; Avouris, Ph.; Pan, Z. W.; Wang, Z. L. *J. Phys. Chem. B* **2003**, *107*, 659.
- (6) Comini, E.; Faglia, G.; Pan, Z. W.; Wang, Z. L. *Appl. Phys. Lett.* **2002**, *81*, 1869.
- (7) Bai, X. D.; Wang, E. G.; Gao, P. X.; Wang, Z. L. *Appl. Phys. Lett.* **2003**, *82*, 4806.
- (8) Huges, W.; Wang, Z. L. *Appl. Phys. Lett.* **2003**, *82*, 288.
- (9) Kong, X. Y.; Wang, Z. L. *Nano Lett.* **2003**, *3*, 1625.
- (10) Kissinger, C. D. U.S. Patent 3,327,584.
- (11) Winters, R.; Reinermann, M.; Enss, C.; Weiss, G.; Hunklinger, S. *J. Vac. Sci. Technol. B* **1995**, *13*, 1316.
- (12) Kholkin, A. L.; Wutchrich, Ch.; Taylor, D. V.; Setter, N. *Rev. Sci. Instrum.* **1996**, *67*, 1935.
- (13) Christman, J. A.; Woolcott, R. R., Jr.; Kingon, A. I.; Nemanich, R. *J. Appl. Phys. Lett.* **1998**, *73*, 3851.
- (14) Agronin, A. G.; Rosenwaks, Y.; Rosenman, G. I. *Nano Lett.* **2003**, *3*, 169.
- (15) Yun, W. S.; Urban, J. J.; Gu, Q.; Park, H. K. *Nano Lett.* **2002**, *2*, 447.
- (16) Zavala, G.; Fendler, J. H.; Trolier-McKinstry, S. *J. Appl. Phys.* **1997**, *81*, 7480.
- (17) Harnagea, C.; Pignolet, A.; Alexe, M.; Hesse, D.; Gosele, U. *Appl. Phys. A* **2000**, *70*, 261.
- (18) Mao, S.; Zhao, M.; Wang, Z. L. *Appl. Phys. Lett.* **2003**, *83*, 993.
- (19) Bernardini, F.; Fiorentini, V.; Vanderbilt, D. *Phys. Rev. B* **1997**, *56*, R10 024.
- (20) Kalinin, S. V.; Bonnell, D. A. *Phys. Rev. B* **2002**, *65*, 125408.
- (21) Dunn, S. *Integr. Ferroelectr.* **2003**, *59*, 1505.
- (22) Buhlmann, S.; Dwir, B.; Baborowski, J.; Murali, P. *Appl. Phys. Lett.* **2002**, *80*, 3195.
- (23) Li, J.; Moses, P.; Viehland, D. *Rev. Sci. Instrum.* **1995**, *66*, 215.
- (24) Lefki, K.; Dormans, G. J. M. *J. Appl. Phys.* **1994**, *76*, 1764.
- (25) Lee, W.; Jeong, M. C.; Myoung, J. M. *Nanotechnology* **2004**, *15*, 254.
- (26) Damjanovic, D. *Phys. Rev. B* **1997**, *55*, R649.
- (27) Damjanovic, D. *J. Appl. Phys.* **1997**, *82*, 1788.

NL035198A